Journal of Solid Mechanics Vol. 9, No. 4 (2017) pp. 680-696

Viscous Fluid Flow-Induced Nonlocal Nonlinear Vibration of Embedded DWBNNTs

A. Ghorbanpour Arani [1, 2 *], Z. Khoddami Maraghi [1], R. Kolahchi [1], M. Mohammadimehr[1]

[1]*Faculty of Mechanical Engineering, University of Kashan, Kashan, Iran*
[2]*Institute of Nanoscience & Nanotechnology, University of Kashan, Kashan, Iran*

Received 30 June 2017; accepted 31 August 2017

ABSTRACT

In this article, electro-thermo nonlocal nonlinear vibration and instability of viscous-fluid-conveying double–walled boron nitride nanotubes (DWBNNTs) embedded on Pasternak foundation are investigated. The DWBNNT is simulated as a Timoshenko beam (TB) which includes rotary inertia and transverse shear deformation in the formulation. Considering electro-mechanical coupling, the nonlinear governing equations are derived using Hamilton's principle and discretized based on the differential quadrature method (DQM). The lowest four frequencies are determined for clamped-clamped boundary condition. The effects of dimensionless small scale parameter, elastic medium coefficient, flow velocity, fluid viscosity and temperature change on the imaginary and real components of frequency are also taken into account. Results indicate that the electric potential increases with decreasing nonlocal parameter. It is also worth mentioning that decreasing nonlocal parameter and existence of Winkler and Pasternak foundation can enlarge the stability region of DWBNNT.

Keywords : Nonlinear vibration and instability; DWBNNTs; Pasternak foundation; Conveying viscous fluid; Piezoelasticity theory.

1 INTRODUCTION

BORON nitride nanotubes (BNNTs) show great promise for their mechanical and thermal properties. BNNTs, apart from having high mechanical, electrical and chemical properties, present more resistant to oxidation than carbon nanotubes (CNTs). Hence, they are used for high temperature applications [1,2]. Also, BNNTs are more stable both thermally and chemically [3]. Because of these unique properties, BNNTs have received much attention amongst researchers. It has therefore found multiple applications for BNNTs including mechanical reinforcements and composites, batteries, fuel cell components, transistors and biosensors. The dynamical behaviors of micro/nano structures conveying fluid have been widely reported in the literature. It is noted that most nanodevices can be modeled as a beam [4]. Therefore, investigating the mechanical behaviors of these structures is important in the design of the nanodevices. Single and multi-walled TB models were developed by Wang et al. [5] for the free vibration of CNTs with various end conditions. They concluded that TB model should be used for a better prediction of the frequencies. Nonlocal free vibration problem for micro/nanobeams modeled as a TB theory was studied by Wang et al. [6]. They proposed that the nonlocal effect is more significant at short CNTs. Lu et al. [7] used nonlocal

[*]Corresponding author. Tel.: +98 31 55912450; Fax: +98 31 55912424.
E-mail address: aghorban@kashanu.ac.ir (A.Ghorbanpour Arani).

beam elasticity theory for vibrational properties of CNTs and concluded that nonlocal parameter had a significant effect on the dynamic properties of the beams. Based on the TB theory, Chang and Lee [8] analyzed the effects of flow velocity on the vibration frequency and mode shape of the fluid-conveying single walled carbon nanotube (SWCNT). Their Results indicate that the real component of frequency of a higher mode is always larger than that of a lower mode for different flow velocities. Using DQM, Ke et al. [9] studied nonlocal nonlinear free vibration of embedded double walled carbon nanotubes (DWCNTs) based on the TB theory. They found that an increase in the spring constant of elastic medium leads to higher linear and nonlinear frequencies but lower nonlinear frequency ratio. Using the nonlocal elasticity theory, Mohammadimehr et al. [10] demonstrated the torsional buckling of a DWCNT embedded on Winkler and Pasternak foundations.

They studied the effects of the surrounding elastic medium, the van der Waals (vdW) forces between the inner and the outer nanotubes on the critical torsional buckling load and showed that the shear constant of the Pasternak type increases the nonlocal critical torsional buckling load. Wang et al. [11] developed a micro scale TB model based on strain gradient elasticity theory. Their numerical results reveal that the size effect is only significant when the beam thickness is comparable to the material length scale parameter. Based on the TB theory and Young–Laplace equation, surface effects on the elastic behavior of static bending nanowires were studied by Yan and Jiang [12]. They showed that the surface effects on the stiffness of nanowires are more prominent for slender nanowires. Asghari et al. [13] developed a nonlinear TB model based on the modified couple stress theory and concluded that modeling beams based on the nonlinear and non-classical couple stress formulations results in stiffer behavior than linear and classical formulations.

A new analytically nonlocal TB model is established by Yang et al. [14] for the analysis of the wave propagation in a DWCNTs beam with the nonlocal effects. Their results show that the nonlocal effect on the wave propagations is more significant. Lei et al. [15] investigated the vibrational frequency of DWCNTs, while accounting for surface effects, using the nonlocal TB model. Their results show that the vibrational frequency is significantly affected by the nonlocal parameter, vibration mode and aspect ratio. Based on the nonlocal TB theory and transfer function method, the transverse vibration of the SWCNT-based micro-mass sensor is analyzed by Shen et al. [16]. They showed that the nonlocal TB model is more adequate than the nonlocal Euler-Bernoulli beam (EBB) model for short SWCNT sensors.

None of the researches mentioned above, have considered smart structures such as BNNTs. Recently, considerable attention has been given to investigate the dynamical characteristic of piezoelectric nanotubes. Surface effect on the vibration and buckling behaviors of piezoelectric nanobeams was investigated by Yan and Jiang [17]. They also analyzed the electromechanical coupling and bending behaviors of piezoelectric nanowires considering surface effect. Electro-thermo-mechanical buckling of BNNTs in a polyvinylidene fluoride (PVDF) was investigated by Salehi and Jalili [18] who showed that applying direct and reverse voltages to BNNT changed buckling loads for any axial and circumferential wave-numbers. Ghorbanpour Arani et al. [19,20, 21] illustrated the electro-thermal vibration and buckling behavior of DWBNNTs embedded in an elastic medium using non-local piezo-elastic cylindrical shell theory. They investigated the effects of parameters such as Winkler spring constant, Pasternak shear constant, electric field, and temperature change on the dimensionless natural frequency. It should be pointed out that none of the above mentioned studies have considered the nonlinear higher order terms of strains and electro-mechanical coupling which can enhance the accuracy of the results.

Vibration, buckling and wave propagation in BNNTs has been a topic of great interest in nanomechanics. Due to the lack of study on the nonlinear vibration and instability of DWBNNTs conveying fluid, the present work is motivated on the use of piezoelasticity theory to study the electro-thermo nonlinear vibration and instability response of viscous-fluid-conveying DWBNNTs embedded in a Pasternak foundation. The DWBNNT is modeled as a TB model which is better than the EBB, since the effects of shear deformation and rotary inertia is considered. The couple governing equations are discretized using DQM. The divergence and flutter instability of DWBNNT for the first four modes of resonance frequencies are discussed. Furthermore, the effects of dimensionless small scale, Pasternak foundation, flow velocity, fluid viscosity and temperature change on the frequency and critical fluid velocity are considered.

2 NONLOCAL PIEZOELASTICITY THEORY

Applying an electric field to a piezoelectric material will yield a strain proportional to the displacement field, and vice versa. According to the nonlocal piezoelasticity theory [21], the constitutive equation includes stress σ_{ij} and strain ε_{kl} tensors on the mechanical side, as well as flux density D_m, temperature change T and field strength E_k vectors on the electrostatic side, may be combined as follows [22, 23]

$$(1-(e_0a)^2\nabla^2)\sigma_{ij} = c_{ijkl}\,\varepsilon_{kl} - h_{mij}\,E_m - \lambda_{ij}T \tag{1}$$

$$(1-(e_0a)^2\nabla^2)D_m = h_{mij}\,\varepsilon_{ij} + \in_{mk}^{S}\,E_k - \varsigma_{ij}T \tag{2}$$

where $c_{ijkl}, h_{mij}, \lambda_{ij}, \varsigma_{ij}$ and $\in_{mk}^{S}$ are the elastic stiffnesses, the piezoelectric module, stress-temperature coefficients, pyroelectric constants and the dielectric permittivity constant. Also, e_0a denotes the small scale effect. It is also noted that the electric field E can be written in terms of electric potential ϕ as:

$$E = -\nabla\phi \tag{3}$$

3 MATHEMATICAL MODELING

A schematic diagram of a viscous-fluid-conveying embedded DWBNNT modeled as a TB is shown in Fig. 1 in which geometrical parameters of length L, inner radius R_1, outer radius R_2 and thickness h are also indicated.

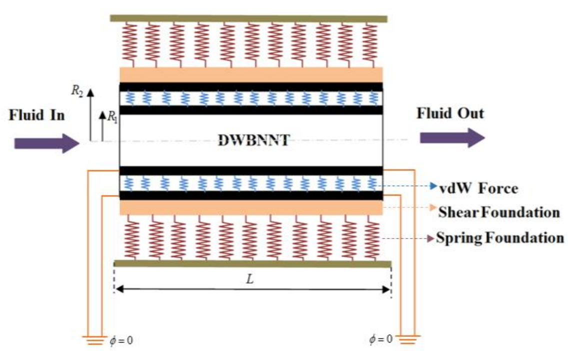

Fig.1
A DWBNNTs conveying viscous fluid embedded in an elastic medium modeled as the nonlocal Timoshenko nanobeam.

Using TB theory, displacement fields are assumed as [9]:

$$\begin{aligned}\tilde{U}_i(x,z,t) &= U_i(x,t) + z\,\psi_i(x,t),\\ \tilde{V}_i(x,z,t) &= 0,\\ \tilde{W}_i(x,z,t) &= W_i(x,t),\end{aligned} \tag{4}$$

where $\tilde{U}_i, \tilde{V}_i$ and $\tilde{W}_i$ denote the longitudinal, circumferential and transverse displacements of the middle surface, respectively. Also, ψ_i is the rotation of beam cross-section and t is time. It is noted that $i=1,2$ represent the inner and outer nanotubes. Using the above equation, the nonlinear strain–displacement von Karman relations are considered as:

$$\varepsilon_{xxi} = \frac{\partial U_i}{\partial x} + \frac{1}{2}\left(\frac{\partial W_i}{\partial x}\right)^2 + z\,\frac{\partial \psi_i}{\partial x}, \tag{5}$$

$$\gamma_{xzi} = \frac{\partial W_i}{\partial x} + \psi_i\,. \tag{6}$$

According to the assumption of TB model, the constitutive relations of DWBNNT can be written as:

$$\sigma_{xxi} - (e_0 a)^2 \frac{\partial^2 \sigma_{xxi}}{\partial x^2} = C_{11}\left\{\frac{\partial U_i}{\partial x} + z\frac{\partial \psi_i}{\partial x} + \frac{1}{2}\left(\frac{\partial W_i}{\partial x}\right)^2\right\} + h_{11}\frac{\partial \varphi_i}{\partial x} - \lambda_{11} T \tag{7a}$$

$$\sigma_{xzi} - (e_0 a)^2 \frac{\partial^2 \sigma_{xzi}}{\partial x^2} = G\left[\frac{\partial W_i}{\partial x} + \psi_i\right] \tag{7b}$$

and

$$D_x - (e_0 a)^2 \frac{\partial^2 D_x}{\partial x^2} = h_{11}\left\{\frac{\partial U_i}{\partial x} + z\frac{\partial \psi_i}{\partial x} + \frac{1}{2}\left(\frac{\partial W_i}{\partial x}\right)^2\right\} + \in_{11}^{s}\frac{\partial \varphi_i}{\partial x} - \varsigma_{11} T \tag{8}$$

where $\lambda_{11} = C_{11}\alpha_x, \varsigma_{11} = h_{11}\alpha_x$ and α_x is the thermal expansion. Using Eqs. (5) and (6), the total electrostatic energy of DWBNNT can be expressed as:

$$\begin{aligned} U = \frac{1}{2}\int_0^l \Bigg\{ & N_{xi}\frac{\partial U_i}{\partial x} + M_{xi}\frac{\partial \psi_i}{\partial x} + \frac{1}{2}N_{xi}\left(\frac{\partial W_i}{\partial x}\right)^2 + Q_{xi}\frac{\partial W_i}{\partial x} + Q_{xi}\psi_i + A_i h_{11}\frac{\partial U_i}{\partial x}\frac{\partial \varphi_i}{\partial x} \\ & + \frac{1}{2}h_{11}A_i\left(\frac{\partial W_i}{\partial x}\right)^2\frac{\partial \varphi_i}{\partial x} - A_i \in_{11}\left(\frac{\partial \varphi_i}{\partial x}\right)^2 - A_i h_{11}\alpha_x T\frac{\partial \varphi_i}{\partial x}\Bigg\} dx \end{aligned} \tag{9}$$

where N_{xi}, M_{xi} and Q_{xi} denote the resultant force, bending moment and transverse shear force, respectively, which can be defined as:

$$N_{xi} = \int_A \sigma_{xxi}\, dA_i, \quad M_{xi} = \int_A \sigma_{xxi} z\, dA_i, \quad Q_{xi} = \int_A \sigma_{xzi}\, dA_i. \tag{10}$$

The kinetic energy of DWBNNT can be written as follows:

$$K_{tube} = \frac{\rho_t A_i}{2}\int_0^L \left[\left(\frac{\partial \tilde{U}_i}{\partial t}\right)^2 + \left(\frac{\partial \tilde{W}_i}{\partial t}\right)^2\right] dx. \tag{11}$$

The work done due to the flowing viscous fluid, surrounding elastic medium and vdW forces can be written as:

$$W = \frac{1}{2}\int_0^L F_{fluid}\big|_z W_1 dx + \frac{1}{2}\int_0^L {}_{fluid}\big|_x U_1 dx + \frac{1}{2}\int_0^L q_1 W_1 dx + \frac{1}{2}\int_0^L q_2 W_2 dx + \frac{1}{2}\int_0^L F_{Elastic\ medium} W_2 dx \tag{12}$$

where F_{fluid} can be obtained by the well-known Navier–Stokes equation as follows [24]:

$$\rho_f \frac{d\vec{V}}{dt} = -\nabla P + \mu \nabla^2 \vec{V} \tag{13}$$

In which P, ρ_f and μ are the static pressure, mass density and viscosity of the flowing fluid, respectively. Also, as can be seen in Fig. 2, velocity field $\vec{V} = (V_x, V_z)$ for the fluid conveying through the inner nanotube for beam model are defined as [25]:

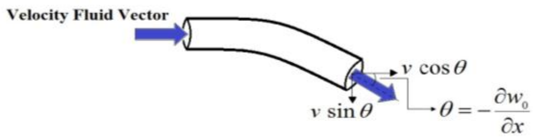

Fig.2
A schematic of nanobeam conveying viscous fluid.

$$V_x=\frac{\partial U_1}{\partial t}+U_f\cos\theta \tag{14}$$

$$V_z=\frac{\partial W_1}{\partial t}-U_f\sin\theta \tag{15}$$

where U_f is the constant velocity of fluid. Hence, substituting Eqs. (14) and (15) into Eq. (13) yields:

$$\frac{\partial P}{\partial x}=-\left[\frac{\partial}{\partial t}+U_f\frac{\partial}{\partial x}\right]\left[\frac{\partial U_1}{\partial t}+U_f\cos\theta\right]+\mu\frac{\partial^2}{\partial x^2}\left[\frac{\partial U_1}{\partial t}+U_f\cos\theta\right] \tag{16a}$$

$$\frac{\partial P}{\partial z}=-\left[\frac{\partial}{\partial t}+U_f\frac{\partial}{\partial x}\right]\left[\frac{\partial W_1}{\partial t}-U_f\sin\theta\right]+\mu\frac{\partial^2}{\partial x^2}\left[\frac{\partial W_1}{\partial t}-U_f\sin\theta\right] \tag{16b}$$

The left side of these equations represents the external force on the nanotube walls due to viscous fluid

$$\left(F_{fluid}\big|_z=\mu\frac{\partial^2}{\partial x^2}\left[\frac{\partial W_1}{\partial t}-U_f\sin\theta\right],F_{fluid}\big|_x=\mu\frac{\partial^2}{\partial x^2}\left[\frac{\partial U_1}{\partial t}+U_f\cos\theta\right]\right)$$

According to the above relations, kinetic energy of flow fluid is given as follow:

$$K_{fluid}=\frac{1}{2}\rho_f\int_0^L\int_{A_f}\left\{\left(\frac{\partial\tilde{U}_1}{\partial t}+U_f\cos\theta\right)^2+\left(\frac{\partial\tilde{W}_1}{\partial t}-U_f\sin\theta\right)^2\right\}dA_f\,dx\,, \tag{17}$$

The second term of Eq. (12) is related to vdW force which can be expressed as:

$$q_1=c(w_2-w_1) \tag{18}$$

$$q_2=-c\frac{R_1}{R_2}(w_2-w_1) \tag{19}$$

where, c is the vdW interaction coefficient. The three term of Eq. (12) is related to the elastic medium. Based on the Winkler and Pasternak foundations, the effect of the surrounding elastic medium on the outer nanotube is written as follows [10]:

$$F_{Elastic\ medium}=-\left(k_W w_2-k_G\nabla^2 w_2\right) \tag{20}$$

where k_W and k_G are Winkler's spring modulus and Pasternak's shear modulus of elastic medium, respectively.

Using Hamilton's principle, the variation form of the equations of motion for the DWBNNT can be written as:

$$\int_0^t \left[\delta K - \delta U + \delta W \right] dt = 0 \tag{21}$$

where $\left(K = K_{tube} + K_{fluid}\right)$. Substituting Eqs. (9), (11) and (12) into Eq. (21) and using the fundamental lemma of the calculus of variation, yields the motion equations for viscous-fluid-conveying embedded DWBNNTs as follows:

δU_1 :

$$\begin{aligned}&-\frac{N_{x1}}{\partial x} - \frac{1}{2} h_{11} A_1 \frac{\partial^2 \varphi_1}{\partial x^2} + (m_1 + m_f) \frac{\partial^2 U_1}{\partial t^2} + U_f m_f \frac{\partial^2 W_1}{\partial x \partial t} \sin\theta + m_f U_f^{\,2} \frac{\partial^2 W_1}{\partial x^2} \sin\theta \\ &= \mu A_f \frac{\partial^3 U_1}{\partial x^2 \partial t} + \mu A_f U_f \frac{\partial^3 W_1}{\partial x^3} \sin\theta - \mu A_f U_f \left(\frac{\partial^2 W_1}{\partial x^2}\right)^2 \cos\theta\end{aligned} \tag{22}$$

δW_1 :

$$\begin{aligned}&-\frac{\partial Q_{x1}}{\partial x} - \frac{\partial N_{x1}}{\partial x} \frac{\partial W_1}{\partial x} - N_{x1} \frac{\partial^2 W_1}{\partial x^2} - \frac{1}{2} A_1 h_{11} \frac{\partial^2 W_1}{\partial x^2} \frac{\partial \phi_1}{\partial x} - \frac{1}{2} A_1 h_{11} \frac{\partial W_1}{\partial x} \frac{\partial^2 \phi_1}{\partial x^2} + m_f \frac{\partial^2 W_1}{\partial t^2} + m_f U_f \frac{\partial^2 U_1}{\partial x \partial t} \sin\theta \\ &- m_f U_f \frac{\partial U_1}{\partial t} \frac{\partial^2 W_1}{\partial x^2} \cos\theta + m_1 \frac{\partial^2 W_1}{\partial t^2} + 2 m_f U_f \frac{\partial^2 W_1}{\partial x \partial t} \cos\theta - m_f U_f \frac{\partial W_1}{\partial t} \frac{\partial^2 W_1}{\partial x^2} \sin\theta - q_1 + m_f U_f^{\,2} \frac{\partial^2 W_1}{\partial x^2} \cos\theta \\ &= \mu U_f A_f \frac{\partial^3 W_1}{\partial x^3} \cos\theta + \mu U_f A_f \left(\frac{\partial^2 W_1}{\partial x^2}\right)^2 \sin\theta + \mu U A_f \frac{\partial^3 W_1}{\partial x^2 \partial t}\end{aligned} \tag{23}$$

$\delta \psi_1$:

$$-\frac{\partial M_{x1}}{\partial x} + Q_{x1} + (I_1 + I_f) \frac{\partial^2 \psi_1}{\partial t^2} = 0 \tag{24}$$

$\delta \phi_1$:

$$h_{11} A_1 \frac{\partial^2 W_1}{\partial x^2} + h_{11} A_1 \frac{\partial^2 W_1}{\partial x^2} \frac{\partial W_1}{\partial x} - 2 \in_{11} A_1 \frac{\partial^2 \phi_1}{\partial x^2} = 0 \tag{25}$$

δU_2 :

$$-\frac{\partial N_{x2}}{\partial x} - \frac{1}{2} h_{11} A_1 \frac{\partial^2 \phi_2}{\partial x^2} + m_2 \frac{\partial^2 U_1}{\partial t^2} = 0 \tag{26}$$

δW_2 :

$$\begin{aligned}&-\frac{\partial Q_{x2}}{\partial x} - \frac{\partial N_{x2}}{\partial x} \frac{\partial W_2}{\partial x} - N_{x2} \frac{\partial^2 W_2}{\partial x^2} - h_{11} A_2 \frac{\partial^2 W_2}{\partial x^2} \frac{\partial \phi_2}{\partial x} \\ &- \frac{1}{2} h_{11} A_2 \frac{\partial W_2}{\partial x} \frac{\partial^2 \phi_2}{\partial x^2} + m_2 \frac{\partial^2 W_2}{\partial t^2} - q_2 + K_w W_2 - G_p \nabla^2 W_2 = 0\end{aligned} \tag{27}$$

$\delta \psi_2$:

$$-\frac{\partial M_{x2}}{\partial x} + Q_{x2} + I_2 \frac{\partial^2 \psi_1}{\partial t^2} = 0 \tag{28}$$

$\delta \phi_2$:

$$h_{11} A_2 \frac{\partial^2 U_2}{\partial x^2} + h_{11} A_2 \frac{\partial^2 W_2}{\partial x^2} \frac{\partial W_2}{\partial x} - 2 \in_{11} A_2 \frac{\partial^2 \phi_2}{\partial x^2} = 0 \tag{29}$$

Using Eqs. (7), (8) and (10), the resultant force, bending moment and transverse shear force can be written as:

$$N_x - (e_0 a)^2 \frac{\partial^2 N_x}{\partial x^2} = C_{11} A \frac{\partial U}{\partial x} + \frac{1}{2} C_{11} A \left(\frac{\partial W}{\partial x}\right)^2 + h_{11} A \frac{\partial \phi}{\partial x} - C_{11} \alpha_x A T \tag{30}$$

$$M_x - (e_0 a)^2 \frac{\partial^2 M_x}{\partial x^2} = C_{11} I \frac{\partial \psi}{\partial x} \tag{31}$$

$$Q_x - (e_0 a)^2 \frac{\partial^2 Q_x}{\partial x^2} = K_s G A \left[\frac{\partial W}{\partial x} + \psi\right] \tag{32}$$

where K_s is shear form factor. The dimensionless parameters for DWBNNTs can be introduced as follows:

$$\begin{array}{llll}
\zeta = \dfrac{x}{l} & (w_i, u_i) = \dfrac{(W_i, U_i)}{r} & \eta_i = \dfrac{l}{r_i} & en = \dfrac{e_0 a}{l} \\
\bar{I}_i = \dfrac{\rho I_i}{\rho A_i r_i^2} & \tau = \dfrac{t}{l}\sqrt{\dfrac{E}{\rho_t}} & u_f = \sqrt{\dfrac{\rho_f}{E}} U_f & \bar{\mu} = \dfrac{\mu}{r\sqrt{E \rho_f}} \\
f_i = \dfrac{EA_f}{EA_i} & \bar{\rho} = \dfrac{\rho_f}{\rho_t} & \bar{\phi} = \dfrac{\phi h_{11}}{lE} & \bar{C}_i = \dfrac{Cl^2}{EA_i} \\
\Delta T = \alpha_x T & \bar{K}_w = \dfrac{K_w l^2}{EA_i} & \bar{G}_p = \dfrac{G_p}{EA_i} & \gamma = \dfrac{\in_{11} E}{h_{11}^2} \\
\gamma = \dfrac{\in_{11} E}{h_{11}^2} & \beta_i = \dfrac{K_{si} G A_i}{EA_i} & \psi = \bar{\psi} &
\end{array} \tag{33}$$

Substituting Eqs. (30) to (33) into Eqs. (22) to (29), one obtains the following governing equations in terms of the mechanical and electrical displacements as:

$$\begin{aligned}
&\delta U_1 : \\
&-\frac{1}{1-\upsilon^2}\frac{\partial^2 u_1}{\partial \xi^2} - \frac{1}{1-\upsilon^2}\frac{1}{\eta_1}\frac{\partial^2 w_1}{\partial \xi^2}\frac{\partial w_1}{\partial \xi} - \frac{3}{2}\eta_1 \frac{\partial^2 \bar{\varphi}_1}{\partial \xi^2} + \frac{1}{2} e_n^2 \eta_1 \frac{\partial^4 \bar{\varphi}_1}{\partial \xi^4} + \left(1+\bar{\rho} f_1\right)\frac{\partial^2 u_1}{\partial \tau^2} - e_n^2 \left(1+\bar{\rho} f_1\right)\frac{\partial^4 u_1}{\partial \xi^2 \partial \tau^2} \\
&-\sqrt{\bar{\rho}} f_1 u_f \frac{1}{\eta_1}\frac{\partial^2 w_1}{\partial \xi \partial \tau}\frac{\partial w_1}{\partial \xi} + e_n^2 \sqrt{\bar{\rho}} f_1 u_f \frac{1}{\eta_1}\frac{\partial^4 w_1}{\partial \xi^3 \partial \tau}\frac{\partial w_1}{\partial \xi} + e_n^2 \sqrt{\bar{\rho}} f_1 u_f \frac{1}{\eta_1}\frac{\partial^2 w_1}{\partial \xi \partial \tau}\frac{\partial^3 w_1}{\partial \xi^3} \\
&-e_n^2 \sqrt{\bar{\rho}} f_1 u_f \left(\frac{1}{\eta_1}\right)^3 \frac{\partial^2 w_1}{\partial \xi \partial \tau}\left(\frac{\partial^2 w_1}{\partial \xi^2}\right)^2 \frac{\partial w_1}{\partial \xi} + 2e_n^2 \sqrt{\bar{\rho}} f_1 u_f \frac{1}{\eta_1}\frac{\partial^3 w_1}{\partial \xi^2 \partial \tau}\frac{\partial^2 w_1}{\partial \xi^2} - f_1 u_f^2 \frac{1}{\eta_1}\frac{\partial^2 w_1}{\partial \xi^2}\frac{\partial w_1}{\partial \xi} + e_n^2 f_1 u_f^2 \frac{\partial^4 w_1}{\partial \xi^4}\frac{\partial w_1}{\partial \xi} \\
&+3e_n^2 f_1 u_f^2 \frac{1}{\eta_1}\frac{\partial^2 w_1}{\partial \xi^2}\frac{\partial^3 w_1}{\partial \xi^3} - e_n^2 f_1 u_f^2 \left(\frac{1}{\eta_1}\right)^3 \left(\frac{\partial^2 w_1}{\partial \xi^2}\right)^3 \frac{\partial w_1}{\partial \xi} - \bar{\mu}\sqrt{\bar{\rho}} f_1 \frac{1}{\eta_1}\frac{\partial^3 u_1}{\partial \xi^2 \partial \tau} + e_n^2 \sqrt{\bar{\rho}}\bar{\mu} f_1 \frac{1}{\eta_1}\frac{\partial^5 u_1}{\partial \xi^4 \partial \tau} \\
&+f_1 \bar{\mu} u_f \left(\frac{1}{\eta_1}\right)^2 \left\{\frac{\partial^3 w_1}{\partial \xi^3}\frac{\partial w_1}{\partial \xi} - e_n^2 \frac{\partial^5 w_1}{\partial \xi^5}\frac{\partial w_1}{\partial \xi} - e_n^2 \left(\frac{\partial^3 w_1}{\partial \xi^3}\right)^2 + 6e_n^2 \left(\frac{1}{\eta_1}\right)^2 \frac{\partial^3 w_1}{\partial \xi^3}\left(\frac{\partial^2 w_1}{\partial \xi^2}\right)^2 \frac{\partial w_1}{\partial \xi} - 2e_n^2 \frac{\partial^4 w_1}{\partial \xi^4}\frac{\partial^2 w_1}{\partial \xi^2}\right. \\
&\left. + \left(\frac{\partial^2 w_1}{\partial \xi^2}\right)^2 - 2e_n^2 \frac{\partial^4 w_1}{\partial \xi^4}\frac{\partial^2 w_1}{\partial \xi^2} - 2e_n^2 \left(\frac{\partial^3 w_1}{\partial \xi^3}\right)^2 + e_n^2 \left(\frac{1}{\eta_1}\right)^2 \left(\frac{\partial^2 w_1}{\partial \xi^2}\right)^4 \right\} = 0
\end{aligned} \tag{34}$$

δW_1 :

$$
\begin{aligned}
&+e_n^2\sqrt{\bar{\rho}}f_1u_f\left(\frac{1}{\eta_1}\right)^2\frac{\partial^4 w_1}{\partial\zeta^4}\frac{\partial w_1}{\partial\zeta}\frac{\partial w_1}{\partial\tau}+3e_n^2\sqrt{\bar{\rho}}f_1u_f\left(\frac{1}{\eta_1}\right)^2\frac{\partial^3 w_1}{\partial\zeta^3}\frac{\partial^2 w_1}{\partial\zeta^2}\frac{\partial w_1}{\partial\tau}\\
&-e_n^2\sqrt{\bar{\rho}}f_1u_f\left(\frac{1}{\eta_1}\right)^4\left(\frac{\partial^2 w_1}{\partial\zeta^2}\right)^3\frac{\partial w_1}{\partial\tau}\frac{\partial w_1}{\partial\zeta}+2e_n^2\sqrt{\bar{\rho}}f_1u_f\left(\frac{1}{\eta_1}\right)^2\left(\frac{\partial^2 w_1}{\partial\zeta^2}\right)^2\frac{\partial^2 w_1}{\partial\zeta\partial\tau}\\
&-\sqrt{\bar{\rho}}f_1u_f\,\frac{1}{\eta_1}\frac{\partial^2 w_1}{\partial\zeta^2}\frac{\partial u_1}{\partial\tau}+e_n^2\sqrt{\bar{\rho}}f_1u_f\,\frac{1}{\eta_1}\frac{\partial^4 w_1}{\partial\zeta^4}\frac{\partial u_1}{\partial\tau}+3e_n^2\sqrt{\bar{\rho}}f_1u_f\,\frac{1}{\eta_1}\frac{\partial^3 w_1}{\partial\zeta^3}\frac{\partial^2 u_1}{\partial\zeta\partial\tau}\\
&+3e_n^2\sqrt{\bar{\rho}}f_1u_f\,\frac{1}{\eta_1}\frac{\partial^2 w_1}{\partial\zeta^2}\frac{\partial^3 u_1}{\partial\zeta^2\partial\tau}-3e_n^2\sqrt{\bar{\rho}}f_1u_f\left(\frac{1}{\eta_1}\right)^3\frac{\partial^3 w_1}{\partial\zeta^3}\frac{\partial^2 w_1}{\partial\zeta^2}\frac{\partial w_1}{\partial\zeta}\frac{\partial u_1}{\partial\tau}\\
&-3e_n^2\sqrt{\bar{\rho}}f_1u_f\left(\frac{1}{\eta_1}\right)^3\left(\frac{\partial^2 w_1}{\partial\zeta^2}\right)^2\frac{\partial w_1}{\partial\zeta}\frac{\partial^2 u_1}{\partial\zeta\partial\tau}-e_n^2\sqrt{\bar{\rho}}f_1u_f\left(\frac{1}{\eta_1}\right)^3\left(\frac{\partial^2 w_1}{\partial\zeta^2}\right)^3\frac{\partial u_1}{\partial\tau}\\
&-\sqrt{\bar{\rho}}f_1u_f\,\frac{1}{\eta_1}\frac{\partial^2 u_1}{\partial\zeta\partial\tau}\frac{\partial w_1}{\partial\zeta}+e_n^2\sqrt{\bar{\rho}}f_1u_f\,\frac{1}{\eta_1}\frac{\partial^4 u_1}{\partial\zeta^3\partial\tau}\frac{\partial w_1}{\partial\zeta}-\bar{\rho}f_1\bar{I}_f\left(\frac{1}{\eta_1}\right)^2\frac{\partial^4 w_1}{\partial\zeta^2\partial\tau^2}\\
&+e_n^2\bar{\rho}f_1\bar{I}_f\left(\frac{1}{\eta_1}\right)^2\frac{\partial^6 w_1}{\partial\zeta^4\partial\tau^2}+f_1u_f^2\frac{\partial^2 w_1}{\partial\zeta^2}-e_n^2f_1u_f^2\frac{\partial^4 w_1}{\partial\zeta^4}-\bar{C}_1w_2+\bar{C}_1w_1+e_n^2\bar{C}_1\frac{\partial^2 w_2}{\partial\zeta^2}\\
&-e_n^2\bar{C}_1\frac{\partial^2 w_1}{\partial\zeta^2}-\sqrt{\bar{\rho}}f_1\bar{\mu}\frac{1}{\eta_1}\frac{\partial^3 w_1}{\partial\zeta^2\partial\tau}+e_n^2\sqrt{\bar{\rho}}f_1\bar{\mu}\frac{1}{\eta_1}\frac{\partial^5 w_1}{\partial\zeta^4\partial\tau}+\bar{\mu}\sqrt{\bar{\rho}}f_1\left(\frac{1}{\eta_1}\right)^2\frac{\partial^3 u_1}{\partial\zeta^2\partial\tau}\frac{\partial w_1}{\partial\zeta}\\
&+7e_n^2f_1u_f\,\bar{\mu}\left(\frac{1}{\eta_1}\right)^3\frac{\partial^4 w_1}{\partial\zeta^4}\frac{\partial^2 w_1}{\partial\zeta^2}\frac{\partial w_1}{\partial\zeta}+7e_n^2f_1u_f\,\bar{\mu}\left(\frac{1}{\eta_1}\right)^3\frac{\partial^3 w_1}{\partial\zeta^3}\left(\frac{\partial^2 w_1}{\partial\zeta^2}\right)^2-4e_n^2f_1u_f\,\bar{\mu}\left(\frac{1}{\eta_1}\right)^5\left(\frac{\partial^2 w_1}{\partial\zeta^2}\right)^4\frac{\partial w_1}{\partial\zeta}\\
&+e_n^2f_1u_f\,\bar{\mu}\left(\frac{1}{\eta_1}\right)^3\frac{\partial^5 w_1}{\partial\zeta^5}\left(\frac{\partial w_1}{\partial\zeta}\right)^2+3e_n^2f_1u_f\,\bar{\mu}\left(\frac{1}{\eta_1}\right)^3\left(\frac{\partial^3 w_1}{\partial\zeta^3}\right)^2\frac{\partial w_1}{\partial\zeta}-4e_n^2f_1u_f\,\bar{\mu}\left(\frac{1}{\eta_1}\right)^5\frac{\partial^3 w_1}{\partial\zeta^3}\left(\frac{\partial^2 w_1}{\partial\zeta^2}\right)^2\left(\frac{\partial w_1}{\partial\zeta}\right)^2\\
&-f_1u_f\,\bar{\mu}\left(\frac{1}{\eta_1}\right)^3\frac{\partial^3 w_1}{\partial\zeta^3}\left(\frac{\partial w_1}{\partial\zeta}\right)^2-f_1u_f\,\bar{\mu}\left(\frac{1}{\eta_1}\right)^3\left(\frac{\partial^2 w_1}{\partial\zeta^2}\right)^2\frac{\partial w_1}{\partial\zeta}-f_1u_f\,\bar{\mu}\left(\frac{1}{\eta_1}\right)^3\left(\frac{\partial^2 w_1}{\partial\zeta^2}\right)^2\frac{\partial w_1}{\partial\zeta}\\
&-e_n^2\bar{\mu}f_1\sqrt{\bar{\rho}}\left(\frac{1}{\eta_1}\right)^2\left[\frac{\partial^5 u_1}{\partial\zeta^4\partial\tau}\frac{\partial w_1}{\partial\zeta}+\frac{\partial^4 u_1}{\partial\zeta^3\partial\tau}\frac{\partial^2 w_1}{\partial\zeta^2}+\frac{\partial^3 u_1}{\partial\zeta^2\partial\tau}\frac{\partial^3 w_1}{\partial\zeta^3}\right]-f_1\bar{\mu}u_f\left(\frac{1}{\eta_1}\right)\frac{\partial^3 w_1}{\partial\zeta^3}\\
&+e_n^2f_1\bar{\mu}u_f\left(\frac{1}{\eta_1}\right)\frac{\partial^5 w_1}{\partial\zeta^5}-4e_n^2f_1\bar{\mu}u_f\left(\frac{1}{\eta_1}\right)^3\frac{\partial^4 w_1}{\partial\zeta^4}\frac{\partial^2 w_1}{\partial\zeta^2}\frac{\partial w_1}{\partial\zeta}-3e_n^2f_1\bar{\mu}u_f\left(\frac{1}{\eta_1}\right)^3\left(\frac{\partial^3 w_1}{\partial\zeta^3}\right)^2\frac{\partial w_1}{\partial\zeta}\\
&+f_1\bar{\mu}u_f\left(\frac{1}{\eta_1}\right)^3\left(\frac{\partial^2 w_1}{\partial\zeta^2}\right)^2\frac{\partial w_1}{\partial\zeta}-6e_n^2f_1\bar{\mu}u_f\left(\frac{1}{\eta_1}\right)^3\frac{\partial^3 w_1}{\partial\zeta^3}\left(\frac{\partial^2 w_1}{\partial\zeta^2}\right)^2+e_n^2f_1\bar{\mu}u_f\left(\frac{1}{\eta_1}\right)^5\left(\frac{\partial^2 w_1}{\partial\zeta^2}\right)^4\frac{\partial w_1}{\partial\zeta}=0
\end{aligned}
\tag{35}
$$

$\delta\psi_1$:

$$
-\frac{\bar{I}_1}{1-\upsilon^2}\left(\frac{1}{\eta_1}\right)^2\frac{\partial^2\bar{\psi}_1}{\partial\zeta^2}+\beta_1\frac{1}{\eta_1}\frac{\partial w_1}{\partial\zeta}+\beta_1\bar{\psi}_1+(\bar{I}_1+\bar{\rho}_f\bar{I}_f)\left(\frac{1}{\eta_1}\right)^2\frac{\partial^2\bar{\psi}_1}{\partial\tau^2}+e_n^2(\bar{I}_1+\bar{\rho}_f\bar{I}_f)\left(\frac{1}{\eta_1}\right)^2\frac{\partial^4\bar{\psi}_1}{\partial\zeta^2\partial\tau^2}=0 \tag{36}
$$

$\delta\phi_1$:

$$
\frac{\partial^2 u_1}{\partial\zeta^2}-e_n^2\frac{\partial^4 u_1}{\partial\zeta^4}+\frac{1}{\eta_1}\frac{\partial^2 w_1}{\partial\zeta^2}\frac{\partial w_1}{\partial\zeta}-e_n^2\frac{1}{\eta_1}\left\{3\frac{\partial^3 w_1}{\partial\zeta^3}\frac{\partial^2 w_1}{\partial\zeta^2}+\frac{\partial w_1}{\partial\zeta}\frac{\partial^4 w_1}{\partial\zeta^4}\right\}-2\eta_1\gamma\frac{\partial^2\phi_1}{\partial\zeta^2}+2e_n^2\eta_1\gamma\frac{\partial^4\phi_1}{\partial\zeta^4}=0 \tag{37}
$$

δU_2 :

$$
-\frac{1}{1-\upsilon^2}\frac{\partial^2 u_2}{\partial\zeta^2}-\frac{1}{\eta_2}\frac{1}{1-\upsilon^2}\frac{\partial^2 w_2}{\partial\zeta^2}\frac{\partial w_2}{\partial\zeta}+\frac{1}{2}e_n^2\eta_2\frac{\partial^4\bar{\varphi}_2}{\partial\zeta^4}+\frac{\partial^2 u_2}{\partial\tau^2}-e_n^2\frac{\partial^4 u_2}{\partial\zeta^2\partial\tau^2}-\frac{3}{2}\eta_2\frac{\partial^2\bar{\phi}_2}{\partial\zeta^2}=0 \tag{38}
$$

$$
\begin{aligned}
&\delta W_2: \\
&-\beta_2\frac{\partial^2 w_1}{\partial\zeta^2}-\eta_2\beta_2\frac{\partial\bar{\psi}_2}{\partial\xi}-\frac{1}{\eta_2}\frac{\partial^2 u_2}{\partial\tau^2}\frac{\partial w_2}{\partial\zeta}+e_n^2\frac{1}{\eta_2}\left\{\frac{\partial^4 u_2}{\partial\zeta^2\partial\tau^2}+2\frac{\partial^3 u_2}{\partial\zeta\partial\tau^2}\frac{\partial^2 w_2}{\partial\zeta^2}+\frac{\partial^2 u_2}{\partial\tau^2}\frac{\partial^3 w_2}{\partial\zeta^3}\right\} \\
&-\frac{1}{1-\upsilon^2}\frac{1}{\eta_2}\frac{\partial u_2}{\partial\zeta}\frac{\partial^2 w_2}{\partial\zeta^2}+e_n^2\frac{1}{1-\upsilon^2}\frac{1}{\eta_2}\left\{\frac{\partial^3 u_2}{\partial\zeta^3}\frac{\partial^2 w_2}{\partial\zeta^2}+2\frac{\partial^2 u_2}{\partial\zeta^2}\frac{\partial^3 w_2}{\partial\zeta^3}+\frac{\partial u_2}{\partial\zeta}\frac{\partial^4 w_2}{\partial\zeta^4}\right\} \\
&-\frac{1}{2}\frac{1}{1-\upsilon^2}\left(\frac{1}{\eta_2}\right)^2\left(\frac{\partial w_2}{\partial\zeta}\right)^2\frac{\partial^2 w_2}{\partial\zeta^2}+e_n^2\left(\frac{1}{\eta_2}\right)^2\left\{3\frac{\partial^3 w_2}{\partial\zeta^3}\frac{\partial^2 w_2}{\partial\zeta^2}\frac{\partial w_2}{\partial\zeta}+\left(\frac{\partial^2 w_2}{\partial\zeta^2}\right)^3+\frac{1}{2}\left(\frac{\partial w_2}{\partial\zeta}\right)^2\frac{\partial^4 w_2}{\partial\zeta^4}\right\} \\
&+\frac{\overline{\Delta T}}{1-\upsilon^2}\frac{\partial^2 w_2}{\partial\zeta^2}-e_n^2\frac{\overline{\Delta T}}{1-\upsilon^2}\frac{\partial^4 w_2}{\partial\zeta^4}-\frac{1}{2}e_n^2\frac{\partial^3\bar{\phi}_2}{\partial\zeta^3}\frac{\partial^2 w_2}{\partial\zeta^2}+\frac{\partial^2 w_2}{\partial\tau^2}-e_n^2\frac{\partial^4 w_2}{\partial\zeta^2\partial\tau^2}+\bar{K}_w w_2-e_n^2\bar{K}_w\frac{\partial^2 w_2}{\partial\zeta^2} \\
&-\bar{G}_p\frac{\partial^2 w_2}{\partial\zeta^2}+e_n^2\bar{G}_p\frac{\partial^4 w_2}{\partial\zeta^4}-\bar{C}_2 w_1+e_n^2\bar{C}_2\frac{\partial^2 w_1}{\partial\zeta^2}+\bar{C}_2 w_2-e_n^2\bar{C}_2\frac{\partial^2 w_2}{\partial\zeta^2}-\frac{3}{2}\frac{\partial^2 w_2}{\partial\zeta^2}\frac{\partial\bar{\phi}_2}{\partial\zeta} \\
&+\frac{3}{2}e_n^2\left\{\frac{\partial^4 w_2}{\partial\zeta^4}\frac{\partial\bar{\phi}_2}{\partial\zeta}+2\frac{\partial^3 w_2}{\partial\zeta^3}\frac{\partial^2\bar{\phi}_2}{\partial\zeta^2}+\frac{\partial^2 w_2}{\partial\zeta^2}\frac{\partial^3\bar{\phi}_2}{\partial\zeta^3}\right\}=0
\end{aligned}
\tag{39}
$$

$$
\begin{aligned}
&\delta\psi_2: \\
&-\frac{\bar{I}_2}{1-\upsilon^2}\left(\frac{1}{\eta_2}\right)^2\frac{\partial^2\bar{\psi}_2}{\partial\zeta^2}+\beta_2\frac{1}{\eta_2}\frac{\partial w_2}{\partial\zeta}+\beta_2\bar{\psi}_2+(\bar{I}_2+\bar{\rho}_f\bar{I}_f)\left(\frac{1}{\eta_2}\right)^2\frac{\partial^2\bar{\psi}_2}{\partial\tau^2}+e_n^2(\bar{I}_2+\bar{\rho}_f\bar{I}_f)\left(\frac{1}{\eta_2}\right)^2\frac{\partial^4\bar{\psi}_2}{\partial\zeta^2\partial\tau^2}=0
\end{aligned}
\tag{40}
$$

$$
\begin{aligned}
&\delta\phi_2: \\
&\frac{\partial^2 u_2}{\partial\zeta^2}-e_n^2\frac{\partial^4 u_2}{\partial\zeta^4}+\frac{1}{\eta_2}\frac{\partial^2 w_2}{\partial\zeta^2}\frac{\partial w_2}{\partial\zeta}-e_n^2\frac{1}{\eta_2}\left\{3\frac{\partial^3 w_2}{\partial\zeta^3}\frac{\partial^2 w_2}{\partial\zeta^2}+\frac{\partial w_2}{\partial\zeta}\frac{\partial^4 w_2}{\partial\zeta^4}\right\}-2\eta_2\gamma\frac{\partial^2\bar{\phi}_2}{\partial\zeta^2}+2e_n^2\eta_2\gamma\frac{\partial^4\bar{\phi}_2}{\partial\zeta^4}=0
\end{aligned}
\tag{41}
$$

4 SOLUTION BY DQM

As can be seen, the motion equations are nonlinear which could not be solved analytically. Hence, DQM is employed which in essence approximates the partial derivative of a function, with respect to a spatial variable at a given discrete point, as a weighted linear sum of the function values at all discrete points chosen in the solution domain of the spatial variable. Let F be a function representing u_i, w_i, ψ_i and φ_i with respect to variable ξ in the following domain of ($0<\xi<L$) having N_ξ grid points along these variable. The *n*th-order partial derivative of $F(\xi)$ with respect to ξ may be expressed discretely [26] at the point (ξ_i) as:

$$
\frac{d^n F(\xi_i)}{d\xi^n}=\sum_{k=1}^{N_\xi}A_{ik}^{(n)}F(\xi_k) \qquad n=1,\ldots,N_\xi-1,
\tag{42}
$$

where $A_{ik}^{(n)}$ is the weighting coefficients associated with *n*th-order partial derivative of $F(\xi)$ with respect to ξ at the discrete point ξ_i whose recursive formulae can be found in. A more superior choice for the positions of the grid points is Chebyshev polynomials as expressed in [26]. According to DQM, mechanical clamped and free electrical boundary conditions at both ends in each layer of DWBNNT may be written as:

$$
u_{i1}=w_{i1}=\phi_{i1}=0, \qquad \sum_{m=1}^{N}C_{2m}^{(1)}w_{im}=0, \qquad at\ \xi=0,
\tag{43}
$$

$$
u_{iN}=w_{iN}=\phi_{iN}=0, \qquad \sum_{m=1}^{N}C_{N-1m}^{(1)}w_{im}=0, \qquad at\ \xi=1.
\tag{44}
$$

Applying these boundary conditions into the governing Eqs. (34-41) yields the following coupled assembled matrix equations

$$\left([K]\begin{pmatrix} d_b \\ d_d \end{pmatrix}+[C]\begin{pmatrix} \dot{d}_b \\ \dot{d}_d \end{pmatrix}+[M]\begin{pmatrix} \ddot{d}_b \\ \ddot{d}_d \end{pmatrix}\right)=0, \tag{45}$$

where d_b and d_d represent boundary and domain points. The $[\mathrm{K}]$,$[\mathrm{C}]$ and $[\mathrm{M}]$ are the stiffness, damping and mass matrices, respectively. For solving the Eq. (45) and reducing it to the standard form of eigenvalue problem, assume that the solution of Eq. (45) has the following form

$$\begin{pmatrix} d_b \\ d_d \end{pmatrix}=\begin{pmatrix} D_b \\ D_d \end{pmatrix}e^{\Omega t}, \tag{46}$$

where D_b and D_d are complex vectors indicating displacements and not depending on time and Ω is frequency of system. By introducing the new vector, we have

$$\begin{pmatrix} W_b \\ W_d \end{pmatrix}=\begin{pmatrix} D_b \\ D_d \end{pmatrix}\Omega. \tag{47}$$

Substituting Eq. (47), it is possible to rewrite Eq. (45) as:

$$\left([K]\begin{pmatrix} D_b \\ D_d \end{pmatrix}+[C]\begin{pmatrix} W_b \\ W_d \end{pmatrix}+\Omega[M]\begin{pmatrix} W_b \\ W_d \end{pmatrix}\right)=0. \tag{48}$$

Eq. (48) can be transformed into

$$\Omega\begin{pmatrix} W_b \\ W_d \end{pmatrix}=-[M]^{-1}[K]\begin{pmatrix} D_b \\ D_d \end{pmatrix}-[M]^{-1}[C]\begin{pmatrix} W_b \\ W_d \end{pmatrix}. \tag{49}$$

Eq. (47) and (49) can be written in the following standard eigenvalue form

$$\Omega\{\mathrm{Z}\}=[\mathrm{A}]\{\mathrm{Z}\}, \tag{50}$$

In which the state vector Z and state matrix $[\mathrm{A}]$ are defined as:

$$\mathrm{Z}=\begin{Bmatrix} \mathrm{D_b} \\ \mathrm{D_d} \\ \mathrm{W_b} \\ \mathrm{W_d} \end{Bmatrix}, \tag{51}$$

and

$$[\mathrm{A}]=\begin{bmatrix} [0] & [\mathrm{I}] \\ -[\mathrm{M}^{-1}\mathrm{K}] & -[\mathrm{M}^{-1}\mathrm{C}] \end{bmatrix}, \tag{52}$$

where $[0]$ and $[\mathrm{I}]$ are the zero and unitary matrices, respectively. However, the frequencies obtained from the solution of Eq. (46) are complex due to the damping existed in the presence of the viscous fluid flow. Hence, the results are containing two real and imaginary parts. The real part is corresponding to the system damping, and the imaginary part representing the system natural frequencies.

5 NUMERICAL RESULTS AND DISCUSSION

In order to obtain the nonlinear frequency and critical fluid velocity for a viscous-fluid-conveying DWBNNT embedded in the Pasternak foundation, a computer program based on the DQM was written, where the effect of dimensionless parameters such as nonlocal parameter, (en), temperature gradient, (ΔT), Winkler, (K_W) and Pasternak,(k_G) modules as well as viscosity of fluid (μ), were investigated. For the purpose of illustration, the DWBNNT dimensions and its mechanical, electrical and thermal properties have been listed in Table 1.

Table 1
Material properties of DWBNNT [10,18, 28]

Thickness	$t=0.075\,nm$
Elastic modulus	$E=1.8\,Tpa$
Poisson ratio	$\upsilon=0.34$
Density	$\rho=3.4870\,gr/cm^3$
Piezoelectric coefficient	$h_{11}=0.95\,C/m$
Dielectric coefficient	$\in_{11}^{s}=1.28\times10^{-8}(F/m)$
Thermal expansion in x direction	$\alpha_x=1.2\times10^{-6}(1/k)$
Inner radius	$R_1=11.43\,nm$
Outer radius	$R_2=12.31\,nm$

Figs. 3 and 4 show the imaginary and real components ($\mathrm{Im}(\omega)$ and $\mathrm{Re}(\omega)$) of dimensionless frequency versus the dimensionless flow velocity (u_f) for the first four modes of resonance frequencies, respectively. It is noted that $\mathrm{Im}(\omega)$ is the resonance frequency and $\mathrm{Re}(\omega)$ is related to the damping. Generally, the system is stable when the real part of the frequency remains zero and it is unstable when the real and imaginary parts of the frequency become positive and zero, respectively. It can be seen that the $\mathrm{Im}(\omega)$ generally decreases with increasing u_f . For zero resonance frequency, DWBNNT becomes unstable and the corresponding fluid velocity is called the critical flow velocity.

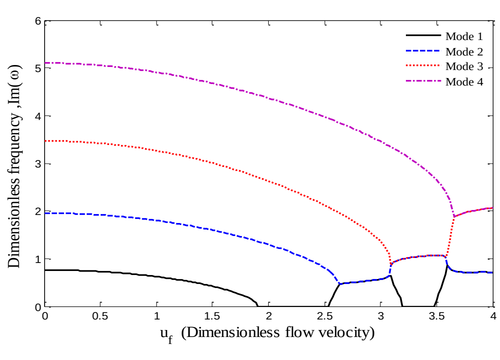

Fig.3
Imaginary part of dimensionless frequency versus dimensionless fluid velocity for the first four modes of DWBNNT.

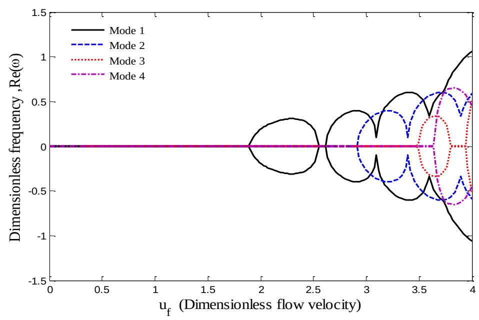

Fig.4
Real part of dimensionless frequency versus dimensionless fluid velocity for the first four modes of DWBNNT.

As can be seen, the critical fluid velocity correspond to the first mode is reached at $u_f \cong 1.91$. This physically implies that the DWBNNT losses its stability due to the divergence via a pitchfork bifurcation while the second, third and fourth modes are still stable. Thereafter, for the fluid velocity within the range $1.91 \le u_f \le 2.53$, the $\mathrm{Re}(\omega)$ of the first mode is positive, which the system becomes unstable. Afterwards, the $\mathrm{Im}(\omega)$ of the first and second modes combines to each other in the region of $2.64 \le u_f \le 3.08$. This physically implies a single coupled-mode between the first and the second modes occurs which is unstable with flutter instability. Also, this phenomenon may be observed in different modes for higher velocities. For example, a coupled-mode between the second and the third modes takes place in the range of $3.11 \le u_f \le 3.59$. Meanwhile, it should be noted that the DWBNNT becomes unstable at second, third and fourth modes when $u_f \cong 2.63, u_f \cong 3.11$ and $u_f \cong 3.65$ respectively. It should also be noted that, the divergence and flutter instability which obtained from the Figs. 3 and 4 are the same as observations made by [29].

Figs. 5 and 6 demonstrate the imaginary and real components of frequency versus the flow velocity for different values of nonlocal parameter (en) in dimensionless form, respectively for the first mode. It is noted that $en = 0$ is corresponding to the classical TB model. As can be seen, the resonance frequency is significantly affected by the en. It is observed that the $\mathrm{Im}(\omega)$ and critical fluid velocity of DWBNNT increase with decreasing of en. Hence, the small scale effect can enlarge the stability region of DWBNNTs. This is perhaps due to the fact that increasing the en decreases interaction force between nanotube atoms, and that leads to a softer structure.

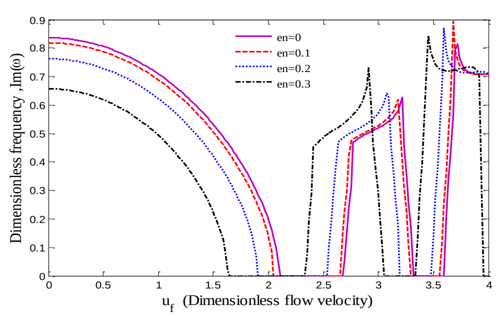

Fig.5
The effect of dimensionless small scale parameter on the imaginary part of dimensionless frequency.

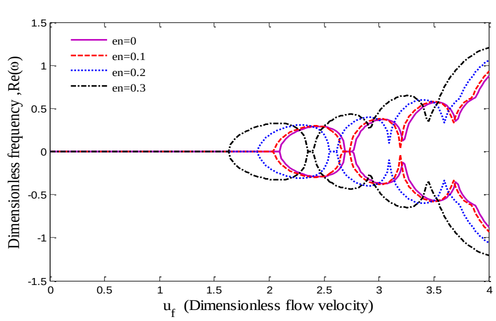

Fig.6
The effect of dimensionless small scale parameter on the real part of dimensionless frequency.

Figs. 7 and 8 illustrate the influence of elastic medium, including Winkler and Pasternak modules, on the $\mathrm{Im}(\omega)$ against u_f for the first mode. As can be seen, existence of Winkler and Pasternak foundation, enlarge the stability region of DWBNNT and increase the resonance frequency. This is perhaps because the beam stiffness increases. It is also concluded that the effect of Pasternak foundation on the resonance frequency and critical fluid velocity is higher than Winkler foundation.

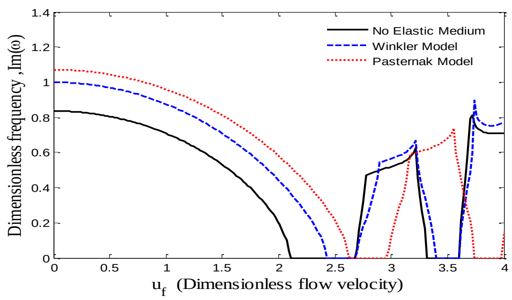

Fig.7
The effect of elastic medium on the imaginary part of dimensionless frequency.

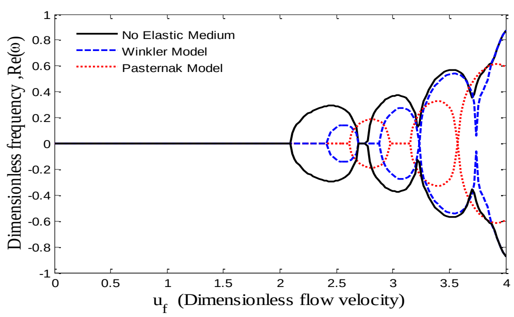

Fig.8
The effect of elastic medium on the real part of dimensionless frequency.

Figs. 9 and 10 illustrate the imaginary component of dimensionless frequency versus dimensionless flow velocity for different values of temperature change in the cases of high and low temperature, respectively. As can be observed from this figure the resonance frequency and critical fluid velocity decrease with increasing of the temperature change at high temperature state. The reason is that a larger temperature change results in more reduction in the nanobeam stiffness. This phenomenon reverses at low (room) temperature state. It should be noted that, this is the same as observations made by [30].

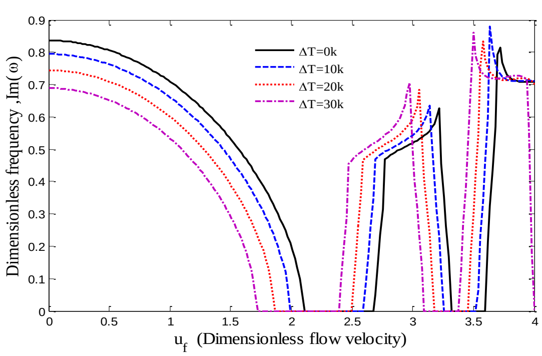

Fig.9
The effect of the temperature change at high temperature state on the dimensionless resonance frequency.

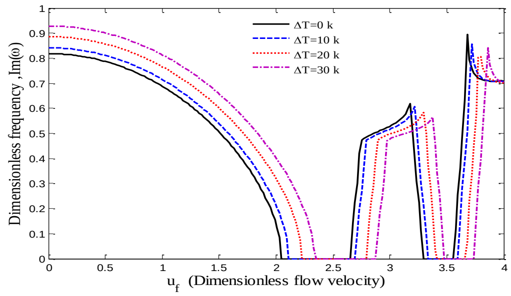

Fig.10
The effect of the temperature change at low temperature state on the dimensionless resonance frequency.

Figs. 11(a) and 11(b) indicate the effect of viscous fluid on the imaginary and real components of frequency in dimensionless form, respectively. It is seen that the effect of viscosity on the dimensionless frequency may be negligible. On the other hands, viscosity of fluid increases the dimensionless frequency very little. This is because increasing viscous parameter increasing shear force on the nanotube. Compared to the work of Wang and Ni [24] who modeled the carbon nanotubes conveying viscous fluid as a continuum structure using the classical EBB theory, in this work, nonlocal vibration of DWBNNT conveying viscous fluid is investigated. However, the results obtained in the present study from Figs. 11(a) and 11(b) are the same as those expressed in Ref. [24].

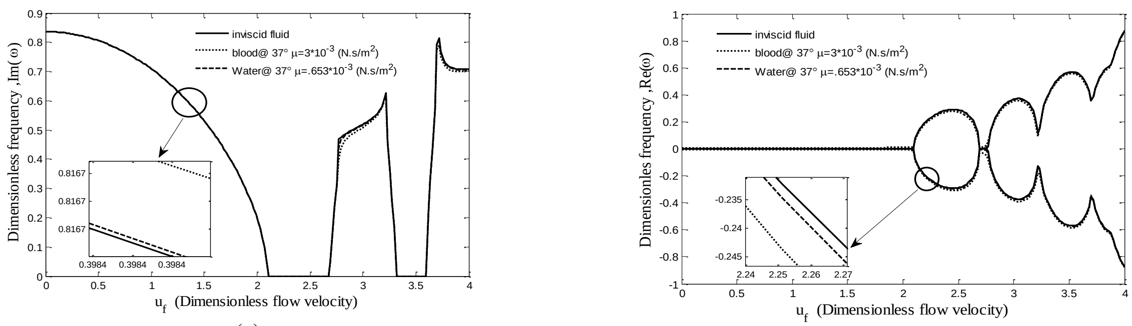

(a) (b)

Fig.11
a)The effect of fluid viscosity on the imaginary part of dimensionless frequency. b)The effect of fluid viscosity on the real part of dimensionless frequency.

Figs. 12 and 13 depict the electric potential along length of nanotube for various u_f and en, respectively. Obviously, electric potentials are constant at the both ends of the beam, satisfying the constant electrical boundary conditions. It can be seen from Figs. 12 and 13 that the electric potential decreases with increasing en, while it increases with increasing u_f. Since, according to specific characteristic of piezoelectric materials, as u_f increases and en decreases, stress and deformation of nanotube increase and subsequently electric potential becomes higher.

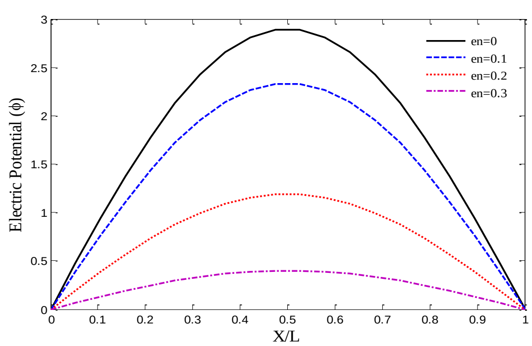

Fig.12
Distribution of electric potential along length of nanotube for various dimensionless small scale parameter.

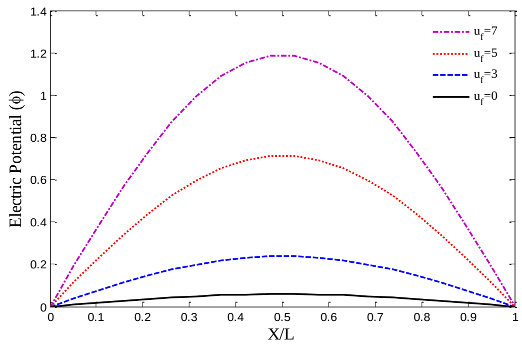

Fig.13
Distribution of electric potential along length of nanotube for various dimensionless fluid velocity.

Imaginary part of dimensionless frequency versus dimensionless flow velocity have been compared for three models in Fig. 14. DWBNNT conveying fluid has been analyzed using EBB theory in Ref. [31] and cylindrical shell model in Ref. [32]. This comparison shows the accuracy of result for three models in which TB theory (present work) is stronger than EBB theory due to consider the shear stress. Also Fig. 14 approves that the result of TB theory is closer to cylindrical shell model in comparison with EBB theory.

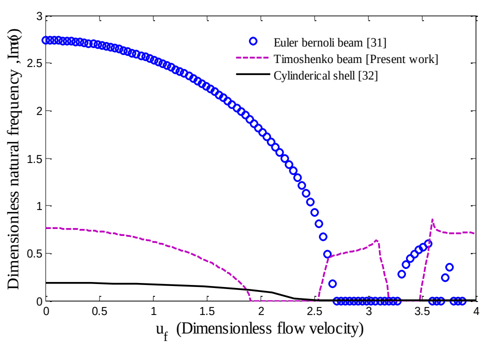

Fig.14
Comparison the results for three models.

6 CONCLUSIONS

Based on the piezoelasticity theory, electro-thermo nonlocal nonlinear vibration and instability of viscous-fluid-conveying DWBNNTs embedded in a Pasternak foundation were investigated. The DWBNNT was modeled as a TB and the vdW forces between the inner and the outer nanotubes were considered. Using DQM the derived governing equations were discretized, and solved to obtain the nonlinear frequency and critical fluid velocity with clamped boundary conditions. The divergence and flutter instability of DWBNNT for the first four modes of resonance frequencies were discussed. The results indicated that decreasing nonlocal parameter and existence of Winkler and Pasternak foundation can enlarge the stability region of DWBNNT. Furthermore, increasing the temperature change at high temperature state, decreases the resonance frequency, while this phenomenon was reverse at low (room) temperature change. Meanwhile, the electric potential decreases with increasing nonlocal parameter, while it increases with an increase of flow velocity. It is also worth mentioning that the effect of fluid viscosity on the frequency was not considerable which was verified when compared with the results obtained by [24].

ACKNOWLEDGMENTS

The author would like to thank the reviewers for their comments and suggestions to improve the clarity of this article. This work was supported by University of Kashan [grant number 574600/39].

REFERENCES

[1] Schwartz M., 2002, *Smart Materials*, John Wiley and Sons, A Wiley-Interscience Publication Inc., New York.

[2] Vang J., 2006, *The Mechanics of Piezoelectric Structures*, World Scientific Publishing Co., USA.

[3] Shahzad Khan M.D., Shahid Khan M., 2011, Computational study of hydrogen adsorption on potassium-decorated boron nitride nanotubes, *International Nano Letters* **1**(8): 103-110.

[4] Yan Z., Jiang L.Y., 2011, The vibrational and buckling behaviors of piezoelectric nanobeams with surface effects, *Nanotechnology* **22**(24): 245703.

[5] Wang C.M., Tan V.B.C., Zhang Y.Y., 2006, Timoshenko beam model for vibration analysis of multi-walled carbon nanotubes, *Journal of Sound and Vibration* **294**(4-5): 1060-1072.

[6] Wang C.M., Zhang Y.Y., He X.Q., 2007, Vibration of nonlocal Timoshenko beams, *Nanotechnology* **18**(10): 105401-105409.

[7] Lu P., Lee H.P., Lu C., Zhang P.Q., 2007, Application of nonlocal beam models for carbon nanotubes, *International Journal of Solids and Structures* **44**(16): 5289-5300.

[8] Chang W.J., Lee H.L., 2009, Free vibration of a single-walled carbon nanotube containing a fluid flow using the Timoshenko beam model, *Physics Letters A* **373**(10): 982-985.

[9] Ke L.L., Xiang Y., Yang J., Kitipornchai S., 2009, Nonlinear free vibration of embedded double-walled carbon nanotubes based on nonlocal Timoshenko beam theory, *Computational Materials Science* **47**(2): 409-417.

[10] Mohammadimehr M., Saidi A.R., Ghorbanpour Arani A., Arefmanesh A., Han Q., 2010, Torsional buckling of a DWCNT embedded on winkler and pasternak foundations using nonlocal theory, *Journal of Mechanical Science and Technology* **24**(6): 1289-1299.

[11] Wang B., Zhao J., Zhou S., 2010, A micro scale Timoshenko beam model based on strain gradient elasticity theory, *European Journal of Mechanics - A/Solids* **29**(4): 591-599.

[12] Jiang L.Y., Yan Z., 2010, Timoshenko beam model for static bending of nanowires with surface effects, *Physica E: Low-dimensional Systems and Nanostructures* **42**(9): 2274-2279.

[13] Asghari M., Kahrobaiyan M.H., Ahmadian M.T., 2010, A nonlinear Timoshenko beam formulation based on the modified couple stress theory, *International Journal of Engineering Science* **48**(12): 1749-1761.

[14] Yang Y., Zhang L., Lim C.W., 2011, Wave propagation in double-walled carbon nanotubes on a novel analytically nonlocal Timoshenko-beam model, *Journal of Sound and Vibration* **330**(8): 1704-1717.

[15] Lei X.W., Natsuki T., Shi J.X., Ni Q.Q., 2012, Surface effects on the vibrational frequency of double-walled carbon nanotubes using the nonlocal Timoshenko beam model, *Composites Part B: Engineering* **43**(1): 64-69.

[16] Shen Z.B., Li X.F., Sheng L.P., Tang G.J., 2012, Transverse vibration of nanotube-based micro-mass sensor via nonlocal Timoshenko beam theory, *Computational Materials Science* **53**(1): 340-346.

[17] Yan Z., Jiang L.Y., 2011, Surface effects on the electromechanical coupling and bending behaviors of piezoelectric nanowires, *Journal of Physics D: Applied Physics* **44**(7): 075404.

[18] Salehi-Khojin A., Jalili N., 2008, Buckling of boron nitride nanotube reinforced piezoelectric polymeric composites subject to combined electro-thermo-mechanical loadings, *Composites Science and Technology* **68**(6): 1489-1501.

[19] Ghorbanpour Arani A., Amir S., Shajari A.R., Mozdianfard M.R., Khoddami Maraghi Z., Mohammadimehr M., 2011, Electro-thermal non-local vibration analysis of embedded DWBNNTs, *Proceedings of the Institution of Mechanical Engineers, Part C* **224**(26): 745-756.

[20] Ghorbanpour Arani A., Kolahchi R., Mosallaie Barzoki A.A., 2011, Effect of material inhomogeneity on electro-thermo-mechanical behaviors of functionally graded piezoelectric rotating cylinder, *Applied Mathematical Modelling* **35**(6): 2771-2789.

[21] Ghorbanpour Arani A., Amir S., Shajari A.R., Mozdianfard M.R., 2012, Electro-thermo-mechanical buckling of DWBNNTs embedded in bundle of CNTs using nonlocal piezoelasticity cylindrical shell theory, *Composites Part B: Engineering* **43**(2): 195-203.

[22] Ghorbanpour Arani A., Shokravi M., Amir S., Mozdianfard M.R., 2012, Nonlocal electro-thermal transverse vibration of embedded fluid-conveying DWBNNTs, *Journal of Mechanical Science and Technology* **26**(5): 1455-1462.

[23] Eringen A.C., 1983, On differential equations of nonlocal elasticity and solutions of screw dislocation and surface waves, *Journal of Applied Physics* **54**(9): 4703-4710.

[24] Wang L., Ni Q., 2009, A reappraisal of the computational modelling of carbon nanotubes conveying viscous fluid, *Mechanics Research Communications* **36**(7): 833-837.

[25] Kuang Y.D., He X.Q., Chen C.Y., Li G.Q., 2009, Analysis of nonlinear vibrations of double-walled carbon nanotubes conveying fluid, *Computational Materials Science* **45**(4): 875-880.

[26] Karami G., Malekzadeh P., 2002, A new differential quadrature methodology for beam analysis and the associated differential quadrature element method, *Computer Methods in Applied Mechanics and Engineering* **191**(32): 3509-3526.

[27] Ke L.L., Wang Y.S., 2011, Flow-induced vibration and instability of embedded double-walled carbon nanotubes based on a modified couple stress theory, *Physica E: Low-dimensional Systems and Nanostructures* **43**(5): 1031-1039.

[28] Mosallaie Barzoki A.A., Ghorbanpour Arani A., Kolahchi R., Mozdianfard M.R., 2012, Electro-thermo-mechanical torsional buckling of a piezoelectric polymeric cylindrical shell reinforced by DWBNNTs with an elastic core, *Applied Mathematical Modelling* **36**(7): 2983-2995.

[29] Ghavanloo E., Daneshmand F., Rafiei M., 2010, Vibration and instability analysis of carbon nanotubes conveying fluid and resting on a linear viscoelastic Winkler foundation, *Physica E: Low-dimensional Systems and Nanostructures* **42**(9): 2218-2224.

[30] Wang L., Ni Q., Li M., Qian Q., 2008, The thermal effect on vibration and instability of carbon nanotubes conveying fluid, *Physica E: Low-dimensional Systems and Nanostructures* **40**: 3179-3182.

[31] Khodami Maraghi Z., Ghorbanpour Arani A., Kolahchi R., Amir S., Bagheri M.R., 2012, Nonlocal vibration and instability of embedded DWBNNT conveying viscose fluid, *Composites Part B: Engineering* **45** (1): 423-432.

[32] Ghorbanpour Arani A., Kolahchi R., Khoddami Maraghi Z., 2013, Nonlinear vibration and instability of embedded double-walled boron nitride nanotubes based on nonlocal cylindrical shell theory, *Applied Mathematical Modelling* **37**(14-15): 7685-7707.